Journal of Medical Case Reports and Reviews
Received 24 Jul 2022 | Revised 26 Jul 2022 | Accepted 24 Sep 2022 | Published Online 30 Sep 2022

DOI: https://doi.org/10.52845/JMCRR/2022/5-9-3
JMCRR 05 (09), 1181–1185

ISSN (O) 2589-8655 | (P) 2589-8647 IF:2.964

Research Article

Super paramagnetic iron oxide-enhanced low-field MRI of liver tumors.

Hama Yukihiro

TECC, Edogawa Hospital,
2-24-18 Edogawa, Tokyo, Japan

Abstract

Background: The advantages of low-field MRI are that there is little image distortion, specific absorption rate can be kept low, and electron return effect can be suppressed, so it can be used not only for interventional radiology, but also for radiation therapy. The purpose of this study was to investigate the visibility of superparamagnetic iron oxides (SPIO)-enhanced low-field MRI for hepatic malignancy.

Materials and Methods: We retrospectively extracted 15 hepatic tumors from 10 patients who underwent SPIO-enhanced MRI at both 0.2T and 1.5T for MRI-guided biopsy or radiofrequency ablation. Tumor-to-liver (T/L) signal intensity ratio (SIR), as well as the SIRs of the aorta-to-background (A/B) and the spleen-to-background (S/B) were calculated and compared between 0.2T and 1.5T MRI using 2D fast low angle shot sequence.

Results: The mean values of T/L SIRs at 0.2T and 1.5T were 4.04 ± 1.96 and 5.08 ± 2.19 (mean ± standard deviation [SD]), respectively ($p = 0.18$). The mean values of A/B SIRs at 0.2T and 1.5T were 174.70 ± 42.89 and 380.36 ±139.18 (mean ± SD), respectively ($p < 0.01$). The mean values of S/B SIRs at 0.2T and 1.5T were 93.58 ±48.13 and 197.28 ± 96.96 (mean ± SD), respectively ($p < 0.01$). Conclusion: Malignant tumors of the liver were clearly visualized on 0.2T low-field MRI after SPIO administration and are comparable to 1.5T high-field MRI.

Keywords: Applied Imaging Technology, Contrast, Hepatobiliary Imaging, Oncologic Imaging, Radiation Oncology Imaging

Supplementary information The online version of this article (https://doi.org/xx.xxx/xxx.xx) contains supplementary material,which is available to autho-rized users.

Corresponding Author:*Kamlesh Dubey* *,MANIPAL UNIVERSITY COLLEGE MALAYSIA (MUCM)*

Introduction

MRI-guided biopsy or radiofrequency ablation (RFA) for liver tumors is highly useful because it allows treatment while monitoring the tumor and the surrounding normal tissue (**1,2**). MRI-guided treatment of liver tumors is usually performed using low-field open MRI. The advantages of low-field MRI are that there is little image distortion, specific absorption rate (SAR) can be kept low, and electron return effect (ERE) can be suppressed, so it can be used not only for interventional radiology, but also for radiation therapy (**3-5**). Disadvantages of low-field MRI include poorer image quality, lower signal-to-noise ratio (SNR), and longer imaging time than high-field MRI.

Superparamagnetic iron oxide (SPIO) is a liver-specific contrast agent that is phagocytosed by Kupffer cells in the liver and helps visualize malignant tumors in the liver (**6**). It may be useful in MRI-guided stereotactic ablative radiotherapy (SABR) because the contrast enhancement effect persists for several days after SPIO administration and SPIO does not have to be administered at each session of SABR. However, the image quality of SPIO-enhanced low-field MRI for hepatic malignant tumors has not been investigated (**7**). The purpose of this study was to investigate the visibility of SPIO-enhanced low-field MRI for hepatic malignancy.

Materials and Methods

All procedures performed in this study were in accordance with the ethical standards of the institutional and/or national research committee and with the 1964 Helsinki Declaration and its later amendments or comparable ethical standards. This study was considered to meet the institutional review board (IRB) waiver conditions of informed consent for clinical investigations involving no more than minimal risk to human subjects. Among liver tumor patients who underwent open MRI-guided biopsy or RFA in the past 10 years, we retrospectively extracted 15 lesions from 10 patients (male/female 7/3) who underwent both SPIO-enhanced 0.2T low-field MRI and 1.5T high-field MRI within 2 hours. The mean ± standard deviation (SD) age was 71.2 ± 6.8 years. Of the 10 cases, 3 had hepatocellular carcinoma, 1 had cholangiocarcinoma, and 6 had liver metastases. Tumors with a maximum diameter of 1 cm or more were selected and evaluated.

Imaging protocols and scanning parameters at 0.2T and 1.5T

All patients underwent SPIO-enhanced MRI (ferucarbotran, Resovist, Bayer Healthcare, Leverkusen, Germany) of liver tumors using a 1.5T MRI unit (Magnetom Vision plus, Siemens, Munich, Germany), and then, the same site was imaged using a 0.2T MRI unit (Magnetom Open viva, Siemens, Munich, Germany) within the next 2 hours. MRI scan parameters are shown in **Table 1**. Sequence parameters were optimized for each scan. Both 0.2T and 1.5T MRI used the 2D fast low angle shot (FLASH) sequence, but 0.2T reduced the flip angle and 1.5T made the echo time (TE) longer.

Table 1: MRI scan parameters at 0.2T and 1.5T

	0.2T MRI	1.5T MRI
Manufacturer's Model Name	MAGNETOM Open viva (Siemens)	MAGNETOM VISION plus (Sieme
Acquisition Type	T1-weighted 2D FLASH	T1-weighted 2D FLASH
Slice Thickness (mm)	10	6
Repetition Time (msec)	31	132
Echo Time (msec)	9	10
Echo Train Length	1	1
Receiver Coil	Body Spine Array Coil	Body Spine Array Coil
Flip Angle	40°	50°
Pixel size (mm)	1.37 x 1.37	1.48 x 1.48

FLASH= fast low angle shot

Comparison of tumor-to-liver signal intensity ratio

To assess the visibility of liver tumors on 0.2T and 1.5T MRI, tumor-to-liver signal intensity ratio (T/L SIR) was calculated by setting regions of interest (ROIs) in the tumor (T) and the surrounding normal liver tissue (L) (**Fig. 1**). T/L SIR was defined as: T/L SIR = T/L. In order to further evaluate the image quality, ROIs were set in the aorta (A), spleen (S) and background (B), and the signal intensity ratios of the aorta-to-background (A/B) and the spleen-to-background (S/B) was calculated respectively. The background signal intensity was defined as an average value of the four corner backgrounds (B1-4): A/B SIR=4*A/Σ(B1-4), S/B SIR=4*S/Σ(B1-4) (**Fig. 1**).

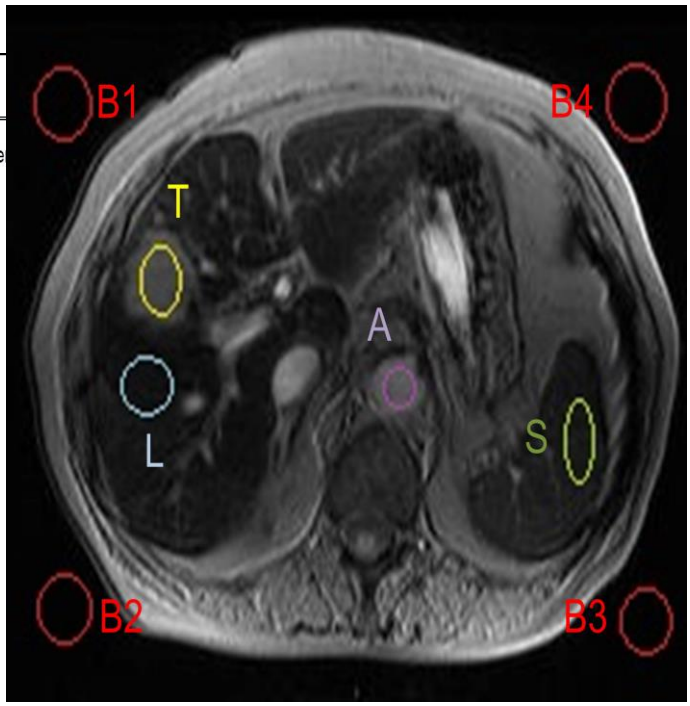

Fig. 1. Assessment of tumor-to-liver signal intensity ratio.

Tumor-to-liver signal intensity ratio was calculated by setting regions of interest (ROIs) in the tumor (T) and the surrounding normal liver tissue (L). ROIs were also set in the aorta (A), spleen (S) and background (B), and the signal intensity ratios of the aorta-to-background (A/B) and the spleen-to-background (S/B) was calculated respectively. The background signal intensity was defined as an average value of the four corner backgrounds (B1-4): A/B SIR=4*A/Σ(B1-4), S/B SIR=4*S/Σ(B1-4).

Statistical analysis

An unpaired *t*-test was used to compare T/L, A/B, and S/B SIRs between 0.2T and 1.5T MRI. A *p*-value that is < 0.05 was considered statistically significant.

Results

Image analysis of 0.2T MRI and 1.5T MRI was possible in all 15 lesions (**Fig. 2**).

Fig. 2a. MRI at 0.2T.

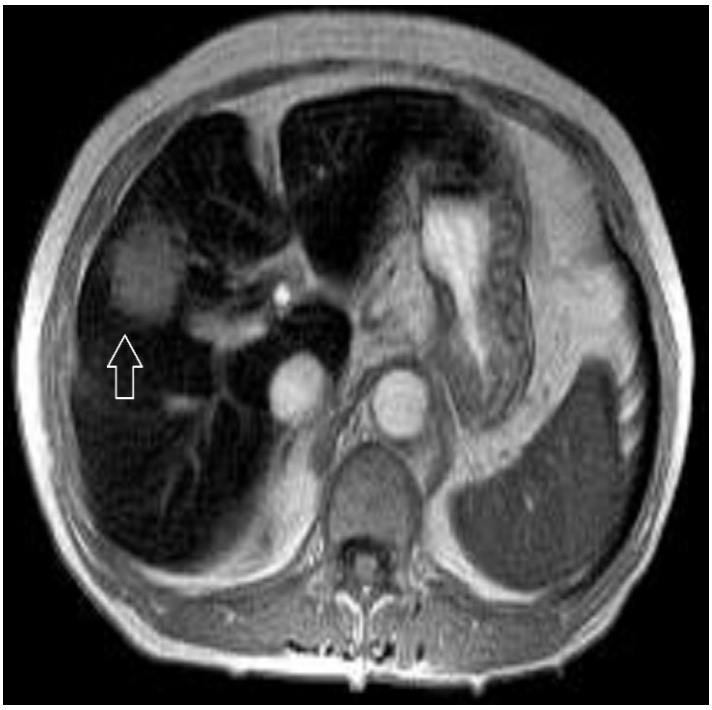

Fig. 2b. MRI at 1.5T.

Fig. 2. SPIO-enhanced 2D fast low angle shot MRI at 0.2T and 1.5T in a patient with cholangiocarcinoma. Liver tumor (arrow) are clearly visualized on both 0.2T (**a**) and 1.5T (**b**) MRI.

The mean values of T/L SIRs at 0.2T and 1.5T were 4.04 ± 1.96 and 5.08 ± 2.19 (mean ± SD), respectively (p = 0.18) (**Fig. 3**). The mean values of A/B SIRs at 0.2T and 1.5T were 174.70 ± 42.89 and 380.36 ±139.18 (mean ± SD), respectively (p < 0.01). The mean values of S/B SIRs at 0.2T and 1.5T were 93.58 ±48.13 and 197.28 ± 96.96 (mean ± SD), respectively (p < 0.01).

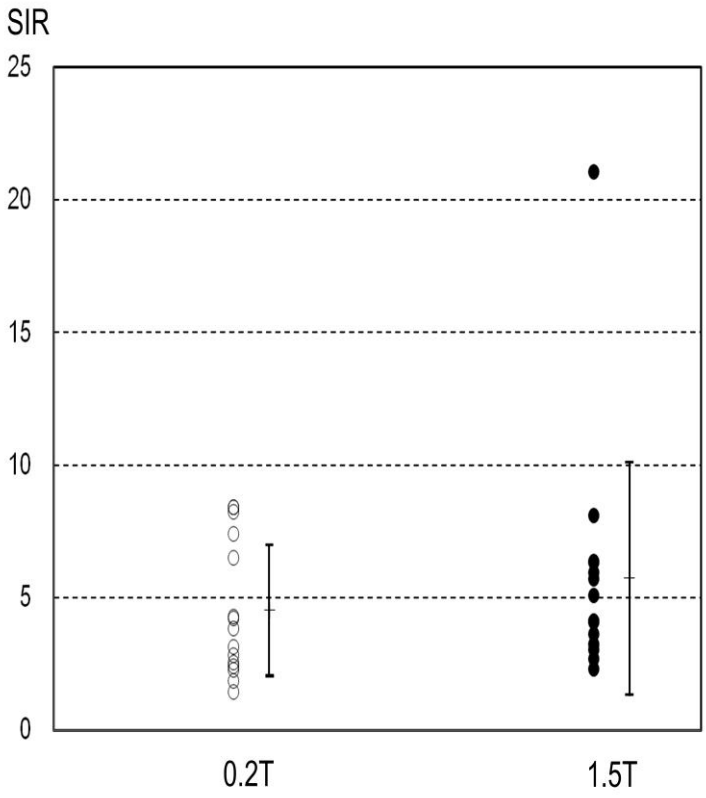

Fig. 3. Tumor-to-liver signal intensity ratio assessed at 0.2T and 1.5T MRI.

Tumor-to-liver signal intensity ratio (SIR) was comparable between 0.2T and 1.5T MRI (p = 0.18).

Discussion

Based on the results of this study, both A/B and S/B SIR were lower at 0.2T than at 1.5T, but T/L SIR was comparable between them. Considering that the SNR of 0.2T MRI is lower than that of 1.5T MRI, it was assumed that A/B and S/B SIRs would be lower at 0.2T. However, the result of the T/L SIR being comparable was not initially expected. The effect of the SPIO is on T2* relaxation and MRI is usually performed using T2-

or T2*-weighted sequences. Since T2*-weighted images can be taken by using long TE sequences, we used long TE FLASH sequence at 1.5T. However, at 0.2T, using long TE sequence significantly reduced SNR and lengthened the imaging time, therefore long TE sequence could not be used. We optimized the sequence parameters by lowering the flip angle (FA) and making the slice thickness 10 mm to shorten the imaging time while maintaining the SNR at 0.2T. As far as we know, this is the first report that has evaluated the imaging performance of SPIO-enhanced liver tumors at 0.2T compared to 1.5T MRI. Since the T/L SIR was comparable at 0.2T and 1.5T, SPIO-enhanced MRI may be feasible for imaging liver tumors even in a low-field MRI.

At present, there is no consensus on pulse sequences for monitoring liver tumors during MRI-guided radiotherapy (**8,9**). SPIO was found to be useful in visualizing liver tumors because it causes strong spin-spin interactions not only in 1.5T high-field MRI but in 0.2T low-field one. If low-field MRI can be used to accurately monitor liver tumors during radiotherapy, ERE can be suppressed even if there is an intestinal tract near the tumor, making it possible to achieve safer radiotherapy (**5**). So far, there has been only one case report in the literature that attempted to visualize a liver tumor during radiotherapy using a liver-specific contrast agent (**10**). However, since linear gadolinium-based contrast agent (GBCA) was used in the past report, long-term toxicity such as nephrogenic systemic fibrosis and neuronal deposition is a concern. It is considered safer to use SPIO than to use linear GBCA in MRI-guided radiotherapy for liver tumors.

Some limitations should be noted in this study. First, this is a retrospective study of patients with liver tumors who underwent MRI-guided interventional procedures rather than MRI-guided radiotherapy. We think that the research using the MRI-guided radiotherapy system actually used in clinical practice will draw a more practical conclusion. However, the currently available low-field MRI-guided radiotherapy system does not allow us to customize the MRI sequence parameters. Second, we analyzed only those liver tumors that were clearly visualized on low-field MRI. Therefore, it should be noted that there is a selection bias in this study. However, even if the selection bias exists, this study is the first report to show the feasibility of SPIO-enhanced MRI at 0.2T. It would be expected to be applied in low-field MRI-guided radiotherapy.

Conclusion

In conclusions, liver tumors were clearly visualized by using liver-specific SPIO even in low magnetic field MRI. Imaging of liver tumors with SPIO may also be applicable to low-field MRI-guided radiotherapy.

References

1. Goldberg SN, Grassi CJ, Cardella JF, Charboneau JW, Dodd 3rd GD, Dupuy DE, et al, Society of Interventional Radiology Technology Assessment Committee; International Working Group on Image-Guided Tumor Ablation. Image-guided tumor ablation: standardization of terminology and reporting criteria. *Radiology* 2005;235:728-39.

2. Freedman JN, Collins DJ, Bainbridge H, Rank CM, Nill S, Kachelrieß M, et al. T2-Weighted 4D Magnetic Resonance Imaging for Application in Magnetic

Resonance-Guided Radiotherapy Treatment Planning. *Invest Radiol* 2017;52:563-73.

3. Marques JP, Simonis FFJ, Webb AG. Low-field MRI: An MR physics perspective. *J Magn Reson Imaging* 2019;49:1528-42.

4. Gach HM, Curcuru AN, Wittland EJ, Maraghechi B, Cai B, Mutic S, et al. MRI quality control for low-field MR-IGRT systems: Lessons learned. *J Appl Clin Med Phys* 2019;20:53-66.

5. Raaijmakers AJE, Raaymakers BW, Lagendijk JJW. Magnetic-field-induced dose effects in MR-guided radiotherapy systems: dependence on the magnetic field strength. *Phys Med Biol* 2008;53:909-23.

6. Knobloch G, Colgan T, Wiens CN, Wang X, Schubert T, Hernando D, et al. Relaxivity of Ferumoxytol at 1.5 T and 3.0 T. *Invest Radiol* 2018;53:257-63.

7. Mendiratta-Lala M, Masch WR, Shampain K, Zhang A, Jo AS, Moorman S, et al. MRI assessment of hepatocellular carcinoma after local-regional therapy: A comprehensive review. *Radiology: Imaging Cancer* 2020;2:e190024.

8. Paganelli C, Lee D, Kipritidis J, Whelan B, Greer PB, Baroni G, et al. Feasibility study on 3D image reconstruction from 2D orthogonal cine-MRI for MRI-guided radiotherapy. *J Med Imaging Radiat Oncol* 2018;62:389-400.

9. Hama Y, Tate E. SPIO-enhanced 0.35T MRI-guided radiotherapy for liver malignancies: usefulness in tumor visualization. *Br J Radiol* 2022;95:20211131. doi: 10.1259/bjr.20211131.

10. Wojcieszynski AP, Rosenberg SA, Brower JV, Hullett CR, Geurts MW, Labby ZE, et al. Gadoxetate for direct tumor therapy and tracking with real-time MRI-guided stereotactic body radiation therapy of the liver. *Radiother Oncol* 2016;118:416-8.